Tight-binding study of the {113} planar interstitial defects in Si

Masanori Kohyama
Department of Material Physics, Osaka National Research Institute, Agency of Industrial Science and Technology, 1-8-31, Midorigaoka, Ikeda, Osaka 563, Japan

Seiji Takeda
Department of Physics, Osaka University, 1-16, Machikaneyama, Toyonaka, Osaka, 560, Japan

(Received 1 September 1994; revised manuscript received 27 December 1994)

The atomic and electronic structure of the {113} planar interstitial defects in Si has been examined by using the transferable semiempirical tight-binding method, based on the reconstructed atomic model. The present results quantitatively confirm our previous conclusion obtained by use of the Stillinger-Weber potential [Phys. Rev. B **46**, 12 305 (1992)] regarding the energy and atomic structure. The features of the electronic structure resemble those of reconstructed ⟨110⟩ tilt boundaries in Si. There exist no electronic states inside the minimum band gap in accordance with the small bond distortions, although defect-localized states are generated, especially at the conduction-band edge. Large portions of such localized states exist at the eight-membered rings and neighboring five-membered rings. Effects of bond distortions, odd-membered rings, and hexagonal six-membered rings at the defects on the local electronic structure have been observed, which are essentially consistent with those found in calculations of grain boundaries in Si. Possible origins of the gap states associated with the {113} defects have been discussed.

I. INTRODUCTION

Elucidation of the atomic structure and mechanism of generation of the {113} planar defects in Si or Ge has been one of the long-standing difficult problems in the field of lattice defects in semiconductors.[1–4] The {113} planar or rodlike defects are induced by electron irradiation, ion implantation, or thermal annealing only in Si or Ge. The defects are considered to consist of an aggregation of supersaturated self-interstitials, because the defects often exhibit unfaulting into perfect dislocation loops of interstitial type. However, it is very strange that interstitial atoms are aggregated not on simple planes such as {111}, {110}, or {100}, but on {113} planes.

Recently, this difficult problem has been solved by an effective combination of experiments using high-resolution transmission electron microscopy (HRTEM) and theoretical calculations.[5–10] By using ⟨110⟩ cross-sectional HRTEM observations in Si (Ref. 5) and Ge,[6,7] an atomic model has been constructed.[5] The model is described by an arrangement of two kinds of structural units, *I* and *O* units, on the {113} plane. These units consist of atomic rings without any coordination defects, similar to those in reconstructed ⟨110⟩ tilt boundaries in Si or Ge.[11] An *I* unit contains a self-interstitial atom chain along the ⟨110⟩ direction. The core of this unit corresponds to a tiny rod of hexagonal Si. An *O* unit contains an eight-membered ring and contains no interstitial atoms. In the observed sequence of units along the ⟨332⟩ direction, the ratio of *I* units is 62% in Si (Ref. 5) and 65% in Ge,[6] and there exists no long-range periodicity. However, some short-range order is observed. For example, *O* units are arranged separately at intervals of one or two *I* units, occasionally three *I* units. These observations and the model are consistent with the observed electron-diffraction patterns.[12]

On the theoretical side, we have examined[8] the stability of the proposed atomic model by energy-minimization calculations using an empirical interatomic potential for Si, the Stillinger-Weber (SW) potential.[13] It has been shown that the models, in which the arrangement and composition of structural units are similar to the observed structure, can exist stably with relatively small bond distortions and with much smaller energy per interstitial atom than that of an isolated self-interstitial in bulk Si. Calculations[14] using another kind of interatomic potential[15] have also shown the relative stability of a similar model. Further, our calculations of various models[8] have shown that *I* units are more stable when neighboring side by side on the {113} plane than isolated *I* units, and that the insertion of *O* units can stabilize the sequence of *I* units. These points induce the mechanism of generation of the planar defects and the origin of the observed arrangement of the units. Recently, it has been shown that the calculated configurations coincide well with HRTEM observations,[9,10] and a generalized view of the structure and mechanism of generation of the {113} defects has been discussed from a viewpoint of successive nucleation of *I* units, namely line interstitial defect (LID) structures.[10]

In this paper,[16] the atomic and electronic structure of the {113} planar defects is examined by using the tight-binding electronic theory. The quantitative reliability of empirical potentials is not enough in cases with large bond distortions or coordination defects, because such potentials do not directly deal with electronic structure. In addition, the SW potential regards the energy difference between diamond Si and hexagonal Si as being zero, although this value is indeed very small. In this paper, we apply the transferable semiempirical tight-binding (SETB) method[17,18] to the same atomic models as our previous ones.[8] This method deals directly with electronic structure, and thus can reproduce energies and atomic structures of complex systems including hexago-

nal Si more quantitatively. Regarding the electronic structure of the {113} defects, it is of much interest to examine the effects of a peculiar atomic configurations; for example, the effects of eight-membered rings, interstitial atom chains, rods of hexagonal Si, odd-membered rings, or bond distortions. It is also of much interest to compare the electronic structure with those of ⟨110⟩ tilt boundaries[19–25] containing similar structural units. Recently, the effects of structural disorder in tilt and twist boundaries in Si have been investigated in detail[23,25] by using the same theoretical method.

II. METHOD OF CALCULATIONS

Energy minimization is performed by using the transferable SETB method for Si.[17,18] This method was developed in order to overcome the weak point of the usual SETB method,[22,26] that the transferability of structures of Si other than four-coordinated ones is not necessarily guaranteed. The details of this method were given in Refs. 18 and 24. The binding energy is expressed as a sum of the band-structure energy $E_{\rm bs}$ and the remaining repulsive energy $E_{\rm rep}$. The former is obtained by tight-binding band calculations with the valence atomic-orbital basis, and the latter is given as a sum of short-range repulsive interatomic potentials. As compared with the usual SETB method, the behavior of the two-center integrals in the Hamiltonian and that of the interatomic potential are modified for large distances, and these are smoothly truncated. In addition, the dependence on the local environment is incorporated into $E_{\rm rep}$ through the effective coordination numbers. Thus this method can more quantitatively deal with energies and atomic structures of complex systems of Si than the usual SETB method and the SW potential, as discussed in Refs. 18 and 24.

This method also well reproduces electronic structure. However, there exists the weak point that the width of the bulk band gap is slightly overestimated as 2.2 eV, although the valence band and the shape of the dispersion of the lower part of the conduction band can be well reproduced. For self-consistency, an on-site electron repulsion term is included through the form of a Hubbard-like Hamiltonian with the value of U used in Ref. 27, although this effect is not so significant in present systems without any coordination defects.

In this paper, we deal with the $|IO|$ and $|IIO|$ models, following our previous paper.[8] In these models, the structural units sandwiched by "|" are repeated periodically along the ⟨332⟩ direction in addition to the periodicity along the ⟨110⟩ direction for computational convenience. The composition and arrangement of the units in these models resemble the observed structure relatively well,[5] as discussed in Ref. 8. The two-dimensional periodicity on the {113} plane in the $|IO|$ model is a rectangular lattice, although that in the $|IIO|$ model is a face-centered-rectangular lattice because of the different height along the ⟨110⟩ axis in the sequence of the units along the ⟨332⟩ direction.

Three-dimensional supercells are constructed by repeating planar defects periodically along the ⟨113⟩ direction. In the unit cells, 44 net {113} atomic layers are contained, and interstitial atom chains in I units are additionally contained as two central net {113} atomic layers between 22 atomic layers on both sides. Thus the unit cell of the supercell for the $|IO|$ model contains 90 atoms, and that for the $|IIO|$ model contains 136 atoms. In the notation where the X and Y axes are parallel to the ⟨332⟩ and ⟨110⟩ directions in addition to the Z axis along the ⟨113⟩ direction, the primitive vectors of the supercell for the $|IO|$ model are $\mathbf{R}_1=(R_1,0,0)$, $\mathbf{R}_2=(0,R_2,0)$, and $\mathbf{R}_3=(T_x,0,R_3+T_z)$, where $R_1=\sqrt{22}a_0/2$, $R_2=\sqrt{2}a_0/2$, and $R_3=2\sqrt{11}a_0$. T_x and T_z are the components of the rigid-body translation between the two bulk crystals. The primitive vectors for the $|IIO|$ model are $\mathbf{R}_1=(R_x,R_y,0)$, $\mathbf{R}_2=(-R_x,R_y,0)$, and $\mathbf{R}_3=(T_x,0,R_3+T_z)$, where $R_x=3\sqrt{22}a_0/4$, $R_y=\sqrt{2}a_0/4$, and $R_3=2\sqrt{11}a_0$.

Integration over the Brillouin zone of the supercell is performed by using 16 special $\mathbf{k}$ points[28] per irreducible part, which is $\frac{1}{4}$ of the whole zone for both the models. The density of the special $\mathbf{k}$ points has been examined by using the supercell configurations of bulk crystals with the same size and the same periodicity. In lattice relaxation, the symmetric properties of configurations are preserved. Two respective {113} layers in the bulk regions on both sides of the unit cells are fixed at positions with the observed rigid-body translation between the two crystals, $0.032a_0[116]$.[5] The widths of relaxed regions in the unit cells are the same as those in our previous paper. In each step of the relaxation, atomic forces are obtained after the self-consistent iteration, which is terminated if the differences between the input and output occupancies are all kept within 10^{-5} electrons. The relaxation is terminated if all the atomic forces are less than 0.1 eV/Å.

III. RESULTS AND DISCUSSION

In Table I, energy values and bond distortions of relaxed configurations are listed with the previous results[8] using the SW potential under the same rigid-body translation. Table I also lists the results of the {221} $\Sigma=9$ boundary in Si obtained by both the methods[8,24] as a typical reconstructed ⟨110⟩ tilt boundary in Si. Figure 1 shows the relaxed configuration of the $|IIO|$ model.

The energy per aggregated interstitial atom $E_{\rm is}$ is the most proper measure for judging the relative stability as a structure of aggregated self-interstitials. The present values of the two models are much less than the energy of an isolated self-interstitial atom in bulk Si, which is estimated as to be about 4–6 eV by the *ab initio* method,[28] the SW potential,[30] and the tight-binding method.[31] The bond-length and bond-angle distortions in the two models are small, and do not exceed 3% and 25°, respectively, similarly to those in the $\Sigma=9$ boundary. All these results indicate the stability of the present atomic models, which is in good agreement with the previous results. The relaxed configurations are also very similar to the previous ones, which were shown to coincide with the observed HRTEM images and electron-diffraction patterns.[9,10]

Of course, there exists substantial differences between the present and previous results in the absolute energy

TABLE I. Energy values and bond distortions of the relaxed configurations of the $|IO|$ and $|IIO|$ models of the {113} planar defect in Si under the observed rigid-body translation (Ref. 5). E_{is} is the total-energy increase per interstitial atom against the energy of the perfect crystal of the same number of atoms. E_{if} is the interfacial energy. Δr and $\Delta\theta$ indicate the ranges of the bond-length and bond-angle distortions, respectively. Values in the parentheses are those obtained by the SW potential (Ref. 8). Results of the {221} $\Sigma=9$ boundary in Si obtained by the present method (Ref. 24) and by the SW potential (Ref. 8) are also listed.

Models	E_{is} (eV)	E_{if} (J/m^2)	Δr	$\Delta\theta$
$\|IO\|$	0.92	0.60	-1.8% to $+2.8\%$	$-17.9°$ to $+24.0°$
	(1.13)	(0.74)	(-1.4% to $+2.6\%$)	($-18.8°$ to $+22.4°$)
$\|IIO\|$	0.68	0.60	-2.2% to $+1.9\%$	$-20.1°$ to $+23.3°$
	(0.88)	(0.77)	(-2.1% to $+1.7\%$)	($-20.6°$ to $+22.4°$)
$\Sigma=9$ boundary		0.32	-1.6% to $+1.5\%$	$-16.2°$ to $+20.8°$
		(0.45)	(-1.5% to $+1.9\%$)	($-16.3°$ to $+21.2°$)

values. The energy values are overestimated in the SW potential by about 20–30 %, similarly to the case of the $\Sigma=9$ boundary. It should be noted that the energy value of the $\Sigma=9$ boundary by the present method is similar to the results by the usual SETB method[19,21] and by the *ab initio* method,[20] which indicates the quantitative reliability of the present method. On the other hand, the relation between the present values of the two models is similar to the previous one by the SW potential. It is important that the present value of E_{is} for the $|IIO|$ model is much smaller than that for the $|IO|$ model, similarly to the previous results, because the $|IIO|$ model more closely resembles the observed structure with respect to the composition and arrangement of the units. In this way, it can be said that the present results quantitatively support our previous conclusion[8] regarding the energy and atomic structure of the {113} planar defects.

Figure 2 shows the calculated band structure and defect-localized states of the relaxed configuration of the $|IIO|$ model. The band structure is shown along the lines in the two-dimensional Brillouin zone with $k_z=0$, and the defect-localized states are defined by the distribution of wave functions to the atoms of structural units. Of course, the two-dimensional band structure is meaningful only for such periodic configurations. However, it should reveal essential features of electronic structure of the sequence of I and O units with the observed short-range or-

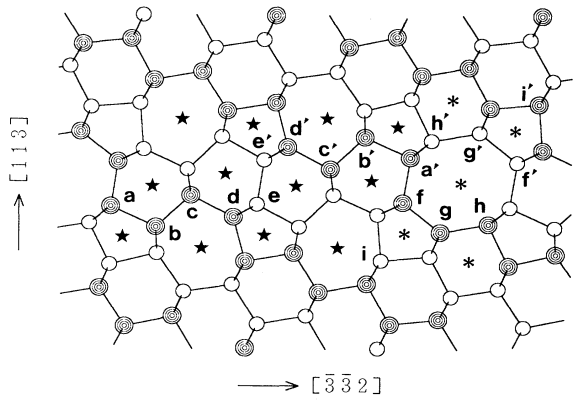

FIG. 1. Relaxed configuration of the $|IIO|$ model of the {113} planar defect in Si. Atomic positions are projected along the ⟨110⟩ direction, and open and closed circles indicate the atoms with the two kinds of heights along the ⟨110⟩ direction. Atomic rings constituting I and O units in one period are indicated by stars and asterisks, respectively. Atoms labeled a–h are those of which the local densities of states (LDOS's) are given in Fig. 3. The atoms labeled a and a', for example, are those symmetrically equivalent to each other.

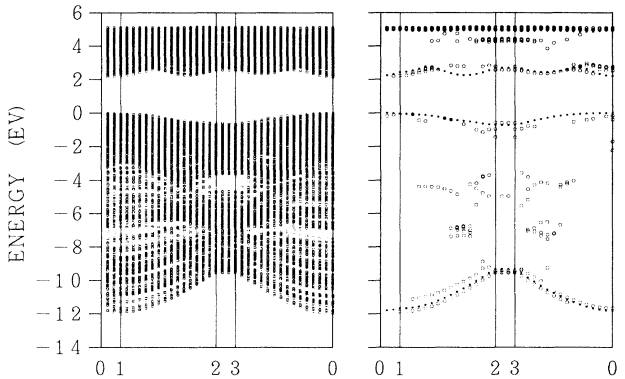

FIG. 2. Band-structure and defect-localized states of the $|IIO|$ model of the {113} planar defect in Si. In the left panel, all the eigenstates are plotted along the lines in the two-dimensional Brillouin zone. In the right panel, the states for which the probability that an electron is located on the atoms of the atomic rings of the structural units exceeds 75% are plotted. The dotted curves indicate the projected band edges of the perfect crystal. Points 0, 1, 2, and 3 correspond to (0,0,0), $(\pi/R_x,0,0)$, $[\pi/R_x,\pi/(2R_y)-\pi R_y/(2R_x^2),0]$, and $[0,\pi/(2R_y)+\pi R_y/(2R_x^2),0]$, respectively, in the Brillouin zone, where $R_x=3\sqrt{22}a_0/4$ and $R_y=\sqrt{2}a_0/4$.

der in the ⟨332⟩ direction.

The essential features of the band structure and localized states in Fig. 2 are similar to those of the $|IO|$ model, and resemble those of the reconstructed ⟨110⟩ tilt boundaries in Si.[19–25] There exist no electronic states inside the minimum band gap between the valence-band maximum and the conduction-band minimum in accordance with the small bond distortions. However, there exist defect-localized states at the band edges, especially at the conduction-band edge, and at the pseudogaps within the valence band as shown in Fig. 2. In the $|IO|$ model,[16] such localized states are remarkable mainly at the conduction-band edge and at the pseudogaps within the valence band. The defect-localized states in both the models resemble the boundary-localized states in the reconstructed ⟨110⟩ tilt boundaries in Si.[19–21,25]

Figure 3 shows the local densities of states (LDOS's) of the atoms in the core region of the $|IIO|$ model. Symmetrically equivalent atoms have the same LDOS's. The LDOS's are calculated by using 32 uniform mesh points in the irreducible part of the Brillouin zone, and are broadened by Gaussians.[23,25] It is possible to examine the origins of the localized states and the effects of structural disorder by analyzing the distribution of wave functions and the LDOS's.

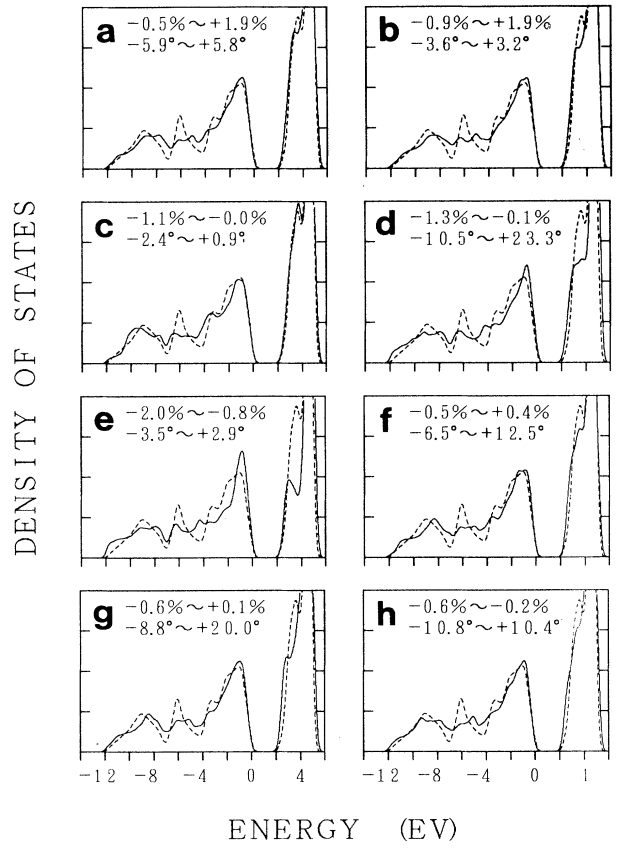

FIG. 3. LDOS's of the atoms in the core region of the $|IIO|$ model of the {113} planar defect in Si. LDOS's of the atoms labeled in Fig. 1 are shown with the ranges of associated bond-length and bond-angle distortions. The dashed lines indicate the bulk density of states, which is the LDOS of the central atom in the bulk region of the supercell.

First, it has been found that large portions of the localized states at the conduction-band edge exist at the eight-membered rings and neighboring five-membered rings in both the models. For example, about the localized state at the conduction band edge at point 2 in Fig. 2, the probability of 55.5% exists among the eight-membered ring, the neighboring five-membered ring containing atoms a, b, and h, and the symmetric five-membered ring containing atoms a', b', and h' in the unit cell in Fig. 1. The sum of the probabilities at atoms h and h' is 14.2%, and the sum of those at the atom neighboring atom b in the five-membered ring and the symmetric atom is 13.6%. Similar distributions have been found for other conduction-band edge states in Fig. 2 and for those in the $|IO|$ model. In one such localized state in the $|IO|$ model, the probability of 70.3% exists among the eight-membered ring and two neighboring five-membered rings equivalent to those in the $|IIO|$ model. The sum of the probabilities at atoms equivalent to atoms h and h' is 20.3%, and that at atoms equivalent to atoms g and g' is 13.8%.

In the $|IIO|$ model, another kind of distribution of the conduction-band-edge state has been found at point 1 in Fig. 2, together with localized states with the above-mentioned kind of distributions. In this state, the probability of 51.5% exists among the five-membered ring containing atoms d and e and the symmetric five-membered ring. The sum of the probabilities at atoms d and d' is the largest; 20.6%.

The distributions of the defect-localized states at the conduction-band edge are consistent with the clear increases at the band edges in LDOS's of atoms d, g, and h in Fig. 3. There seems to exist a tendency that the atoms associated with large bond-angle distortions contain large portions of the localized states at the conduction-band edge, because atoms d, g, and h have relatively large bond-angle distortions. This tendency is also found in the $|IO|$ model, and was found in the $\Sigma=9$ boundary.[25] This is consistent with the general effects of bond distortions found in the calculations of grain boundaries in Si.[25]

However, it should be noted that the present defect-localized states are not sharply localized at specific atoms but exist among the atoms of the structural units, or are not localized along the ⟨110⟩ direction. Thus the origins of the localized states at the conduction-band edge should be the peculiar configurations themselves containing bond-angle distortions and peculiar atomic rings. This is similar to boundary-localized states in the reconstructed ⟨110⟩ tilt boundaries.[21,25]

Second, the localized states at the bottom of the valence band found in the $|IIO|$ model in Fig. 2 should be caused by bond shortening. Large portions of these states exist among atoms with markedly shortened bonds and the neighboring atoms, such as atoms e and e' and atoms of the ordinary six-membered rings in the O unit. These atoms are associated with bond shortening by about 2%. On the other hand, the maximum bond shor-

tening in the $|IO|$ model does not exceed 2%. Localized states at the bottom of the valence band have also been found in calculations of grain boundaries in Si containing shortened bonds,[25] although such bonds are associated with four-membered rings.

Third, there exists a particular kind of change in the shape of the valence-band DOS at many atoms in the core region, especially at atoms *a*, *b*, *f*, and *h* in Fig. 3. In these atoms, the densities are increased at the two minima among the three peaks of the bulk valence-band DOS, namely *s*-like, *s*-*p* mixing, and *p*-like peaks, and decrease at the *s*-*p* mixing peak. Also, the *p*-like peaks are somewhat sharpened. Similar changes are also found in the $|IO|$ model, and were found in the $\Sigma=9$ boundary.[25] This kind of change can be attributed to general effects of odd-membered rings as discussed in Ref. 25, because all atoms with marked changes belong to odd-membered rings. However, this kind of change does not seem to be a simple topological effect, but seems to be related to rather intermediate-range order as discussed in Ref. 25. This is because such changes are markedly not observed at all members of odd-membered rings but at atoms surrounded by several peculiar rings. These changes, coupled with the effects of bond distortions, could be connected with observed changes in the valence-band DOS in amorphous Si by x-ray photoemission spectroscopy (XPS).[32]

Fourth, there exists a local electronic structure similar to that of bulk hexagonal Si at hexagonal six-membered rings of *I* units. The LDOS of atom *e* in Fig. 3 has a striking resemblance to the DOS of bulk hexagonal Si shown in Fig. 4. In both valence-band DOS's as compared with that of bulk diamond Si, the densities are decreased at the *s*-*p* mixing peak and are increased at the valley between the *s*-*p* mixing peak and the *p*-like peak. The *p*-like peak is sharpened by the decrease at the lower side of the peak. A similar resemblance seems to exist at atom *d* in Fig. 3. Similar changes in LDOS's were also observed in calculations of a {111} stacking fault and a {111} $\Sigma=3$ twin boundary in Si (Ref. 22) consisting of arrangements of hexagonal six-membered rings. The DOS of bulk hexagonal Si in Fig. 4 as well as that of bulk diamond Si is well reproduced, as compared with the *ab initio* results.[33]

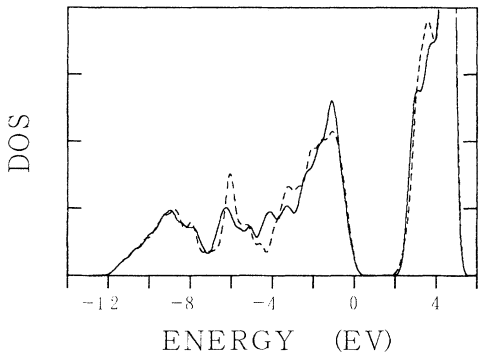

FIG. 4. DOS of bulk hexagonal Si calculated by the present method. The dashed line is that of bulk diamond Si. The first-neighbor distance in the hexagonal structure is equal to that in the equilibrium diamond structure. For the hexagonal structure, 1728 uniform mesh points per whole Brillouin zone have been used, and 2048 uniform mesh points have been used for the diamond structure. The broadening has been performed in a similar way to LDOS's.

However, it should be noted that no LDOS bears a striking resemblance to the DOS of bulk hexagonal Si in the $|IO|$ model. Atoms *d* and *e* in the $|IIO|$ model are located at the center of four hexagonal six-membered rings of two *I* units arranged side by side. It seems that arrangements of hexagonal six-membered rings associated with two or more *I* units arranged side by side are necessary to generate LDOS's bearing a striking resemblance to the DOS of bulk hexagonal Si.

Finally, it should be noted that the present results of electronic structure do not include effects of nonperiodicity in the arrangement of the structural units in the ⟨332⟩ direction, or effects of the edges of planar defects. Concerning the effects of the nonperiodicity, we believe that the present results reveal the essential features of local electronic structure in the observed nonperiodic arrangement of the units with short-range order. This is because essential features of local electronic structure should depend on local environments in Si. Of course, the localization behavior of the defect-localized states along the ⟨332⟩ direction should be enhanced in such nonperiodic arrangements of the units.

Concerning the effects of the edges of planar defects, it can be considered that the edges of arrangements of *I* and *O* units in the ⟨332⟩ direction should contain no deep electronic states in the band gap, because *E* units at the edges should have no coordination defects nor greatly distorted bonds, as shown in our previous paper.[8] However, the edges in the ⟨110⟩ direction may contain coordination defects or greatly distorted bonds, although atomic structures of such edges have not been examined. Thus, if electronic states inside the minimum band gap were associated with the {113} defects, these may be caused by configurations at the edges in the ⟨110⟩ direction. Associated point defects or impurities also may cause such gap states. Nevertheless, it can be concluded that arrangements of *I* and *O* units with the observed short-range order should contain no electronic states inside the minimum band gap, although defect-localized states should exist at the band edges.

IV. SUMMARY

By using the transferable SETB method, we have examined the atomic and electronic structure of the {113} planar defects in Si based on the reconstructed atomic model. Concerning the energy and atomic structure, the present results quantitatively confirm our previous conclusion by the SW potential. The $|IO|$ and $|IIO|$ models are stable with relatively small bond distortions and with much smaller energies per interstitial atom than that of an isolated self-interstitial in bulk Si. The relaxed configurations are very similar to our previous ones, and

the relation between the energy values of the two models is also similar to our previous one, although the SW potential somewhat overestimates the energy values. Concerning the electronic structure, the models have features similar to those of the reconstructed ⟨110⟩ tilt boundaries in Si. There exist no electronic states inside the minimum band gap in accordance with the small bond distortions. However, there exist defect-localized states especially at the conduction-band edge, of which large portions frequently exist among the eight-membered rings and neighboring five-membered rings. We have found the tendency that atoms with large bond-angle distortions contain large portions of such localized states. The effects of bond shortening, odd-membered rings, and hexagonal six-membered rings at the defects on the local electronic structure have also been observed. The present effects of structural disorder are essentially consistent with those found in calculations of grain boundaries in Si. Possible gap states associated with {113} planar defects may be caused by complex structures at the edges of the planar defects in the ⟨110⟩ direction, or by associated point defects or impurities.

[1]M. D. Matthews and S. J. Ashby, Philos. Mag. **27**, 1313 (1973).

[2]C. A. Ferreira Lima and A. Howie, Philos. Mag. **34**, 1057 (1976).

[3]I. G. Salisbury and M. H. Loretto, Philos. Mag. A **39**, 317 (1979).

[4]A. Bourret, in *Microscopy of Semiconducting Materials 1987,* edited by A. G. Cullis and P. D. Augustus, IOP Conf. Proc. No. 87 (Institute of Physics, Bristol, 1987), p. 39.

[5]S. Takeda, Jpn. J. Appl. Phys. **30**, L639 (1991).

[6]S. Takeda, M. Hirata, S. Muto, Guo-Chun Hua, K. Hiraga, and M. Kiritani, Ultramicroscopy **39**, 180 (1991).

[7]S. Takeda, S. Muto, and M. Hirata, Mater. Sci. Formum **83-87**, 309 (1992).

[8]M. Kohyama and S. Takeda, Phys. Rev. B **46**, 12 305 (1992).

[9]S. Takeda and M. Kohyama, in *Microscopy of Semiconducting Materials 1993,* edited by A. G. Cullis and P. D. Augustus, IOP Conf. Proc. No. 134 (Institute of Physics, Bristol, 1993), p. 33.

[10]S. Takeda, M. Kohyama, and K. Ibe, Philos. Mag. A **70**, 287 (1994).

[11]A. Bourret and J. J. Bacmann, Surf. Sci. **162**, 495 (1985); Trans. Jpn. Inst. Met. Suppl. **27**, 125 (1986).

[12]S. Takeda, S. Muto, and M. Hirata, Jpn. J. Appl. Phys. **29**, L1698 (1990).

[13]F. H. Stillinger and T. A. Weber, Phys. Rev. B **31**, 5262 (1985).

[14]A. Parisini and A. Bourret, Philos. Mag. A **67**, 605 (1993).

[15]J. Tersoff, Phys. Rev. B **37**, 6991 (1988).

[16]Preliminary accounts about the tight-binding calculations of the {113} defects have been given in M. Kohyama and S. Takeda, Mater. Sci. Forum **126-128**, 217 (1993); in *Polycrystalline Semiconductors III,* edited by H. P. Strunk, H. J. Werner, O. Bonnaunt, and B. Fortin (Trans Tech, Brookfield, 1994), p. 163.

[17]S. Sawada, Vacuum **41**, 612 (1990).

[18]M. Kohyama, J. Phys. Condens. Matter **3**, 2193 (1991).

[19]R. E. Thomson and D. J. Chadi, Phys. Rev. B **29**, 889 (1984).

[20]D. P. DiVincenzo, O. L. Alerhand, M. Schlüter, and J. W. Wilkins, Phys. Rev. Lett. **56**, 1925 (1986).

[21]M. Kohyama, R. Yamamoto, Y. Watanabe, Y. Ebata, and M. Kinoshita, J. Phys. C **21**, L695 (1988); M. Kohyama, S. Kose, M. Kinoshita, and R. Yamamoto, J. Phys. Condens. Matter **2**, 7809 (1990).

[22]A. T. Paxton and A. P. Sutton, J. Phys. C **21**, L481 (1988); Acta Metall. **37**, 1693 (1989).

[23]M. Kohyama and R. Yamamoto, in *Defect Engineering in Semiconductor Growth, Processing and Device Technology,* edited by S. Ashok, J. Chevallier, K. Sumino, and E. Weber, MRS Symposia Proceedings No. 262 (Materials Research Society, Pittsburgh, 1992), p. 567; in *Amorphous Silicon Technology—1993,* edited by E. A. Schiff, M. J. Thompson, A. Madan, K. Tanaka, and P. G. LeComber, MRS Symposia Proceedings No. 297 (Materials Research Society, Pittsburgh, 1993), p. 177.

[24]M. Kohyama and R. Yamamoto, Phys. Rev. B **49**, 17 102 (1994).

[25]M. Kohyama and R. Yamamoto, Phys. Rev. B **50**, 8502 (1994).

[26]D. J. Chadi, Phys. Rev. Lett. **41**, 1062 (1978); Phys. Rev. B **29**, 785 (1984).

[27]D. Tomanek and M. A. Schlüter, Phys. Rev. Lett. **56**, 1055 (1986); Phys. Rev. B **36**, 1208 (1987).

[28]D. J. Chadi and M. L. Cohen, Phys. Rev. B **8**, 5747 (1973).

[29]R. Car, P. J. Kelly, A. Oshiyama, and S. T. Pantelides, Phys. Rev. Lett. **52**, 1814 (1984).

[30]I. P. Batra, F. F. Abraham, and S. Ciraci, Phys. Rev. B **35**, 9552 (1987).

[31]C. Z. Wang, C. T. Chan, and K. M. Ho, Phys. Rev. Lett. **66**, 189 (1991); I. Kwon, R. Biswas, C. Z. Wang, K. M. Ho, and C. M. Soukoulis, Phys. Rev. B **49**, 7242 (1994).

[32]L. Ley, S. Kowalczyk, R. Pollack, and D.A. Shirley, Phys. Rev. Lett. **29**, 1088 (1972).

[33]F. Zandiehnadem and W. Y. Ching, Phys. Rev. B **41**, 12 162 (1990).